Journal of Molecular Spectroscopy 308-309 (2015) 33–40

Contents lists available at ScienceDirect

Journal of Molecular Spectroscopy

journal homepage: www.elsevier.com/locate/jms

Self- and N_2-broadening of CH_3Br ro-vibrational lines in the ν_2 band: The J and K dependence

Z. Boussetta [a], F. Kwabia Tchana [b,*], H. Aroui [a]

[a] Laboratoire de Dynamique Moléculaire et Matériaux Photoniques, UR11ES03, Université de Tunis, Ecole Nationale Supérieure d'Ingénieurs de Tunis, 5 Av Taha Hussein, 1008 Tunis, Tunisia

[b] LISA, Laboratoire Interuniversitaire des Systèmes Atmosphériques, UMR CNRS 7583, Université Paris-Est Créteil (UPEC) et Université Paris-Diderot (UPD), 61 Avenue du Général de Gaulle, 94010 Créteil Cedex, France

ARTICLE INFO

Article history:
Received 24 July 2014
In revised form 13 December 2014
Available online 24 December 2014

Keywords:
Methyl bromide
CH_3Br
Fourier transform infrared spectroscopy
ν_2 band
Self- and N_2-broadening coefficients
J and K dependence

ABSTRACT

Methyl bromide (CH_3Br) is the major source of inorganic bromine in the atmosphere and contributes significantly to ozone depletion. Indeed, CH_3Br is dissociated by UV radiation, producing Br radicals that catalyze the destruction of ozone. In this paper, we report measured Lorentz self- and N_2-broadening coefficients of CH_3Br in the ν_2 fundamental band using a mono-spectrum non-linear least squares fitting of Voigt profiles which appeared to properly model the observed molecular line shapes within the noise level. These measurements were made by analyzing 12 laboratory absorption spectra recorded at high resolution (0.005, 0.003 or 0.002 cm^{-1}) using the Fourier transform spectrometer Bruker IF125HR located at the LISA facility in Créteil. The spectra were obtained at room temperature using a White-type multipass cell with an optical path of 0.849 m and various pressures. We have been able to determine the self- and N_2-broadening coefficients of 948 ν_2 transitions with quantum numbers as high as $J = 49$ and $K = 10$. The measured self-broadening coefficients range from 0.1542 to 0.4930 cm^{-1} atm^{-1} and the N_2-broadening coefficients range from 0.0737 to 0.1284 cm^{-1} atm^{-1} at 295 K. The accuracy of the broadening coefficients measured in this work is between 4% and 8%, depending on the studied transition. Comparisons with measurements taken in the ν_5 and ν_6 bands of CH_3Br did not show any clear vibrational dependence. The J and K dependences of the self- and N_2-broadening coefficients have been observed and the rotational K dependence has been modeled using empirical polynomial expression. On average, the empirical expression reproduce the measured broadening coefficients to within 6%. The data obtained represent a significant contribution to the determination of broadening coefficients of CH_3Br useful for atmospheric remote sensing and applications.

1. Introduction

Molecular spectroscopy, in the last decades, has become an integral part of both earth atmospheric and interstellar space researches [1,2] and, nowadays, remote sensing measurements using different platforms are valuable tools for detecting and monitoring the composition of the Earth's atmosphere as well as for probing the molecular content of interstellar clouds or the atmospheres of solar and extra-solar objects [2–9]. On the other hand, the successful analysis of atmospheric and astrophysical spectra and the reliability of the retrieved concentration and temperature profiles strongly depend on the accuracy of spectral line parameters, such as line positions, pressure broadening-, shifting-coefficients and integrated absorption coefficients.

With this in mind, laboratory high resolution spectroscopy, being the tool for measuring these parameters, appears as one of the ground building blocks for the achievement of accurate remote sounding methodologies [10–18]. The available spectroscopic data are collected into a number of different databases, such as HITRAN [19], GEISA [20] and JPL [21] which are continuously updated in terms of accuracy, molecular species and spectral coverage. Besides, the study of spectral line shapes is also a rich source of information for shedding light on intermolecular interactions and collision dynamics [22–27].

Methyl bromide (CH_3Br) is one of the molecules included in HITRAN and GEISA, given its relevance in the Earth's atmosphere. Indeed, it plays a relevant role in the chemistry of the Earth's atmosphere, directly entering in the bromine cycle. Methyl bromide has both natural and anthropogenic origins. Its known sources include natural production from oceans [28] and biomass burning [29]. It is also industrially produced for use in agricultural applications and

* Corresponding author. Fax: +33 (0)1 45 17 15 64.
E-mail address: fridolin.kwabia@lisa.u-pec.fr (F. Kwabia Tchana).

http://dx.doi.org/10.1016/j.jms.2014.12.018
0022-2852/

structural fumigations. This molecule significantly contributes to the ozone depletion since CH_3Br is dissociated by UV radiation, producing Br radicals that catalyze the destruction of ozone [30]. These bromine atoms are largely more destructive of ozone than the chlorine atoms coming from the chlorofluorocarbons compounds (CFC) [31]. For this reason, since 2005, the use of CH_3Br has been banned under the Montreal protocol.

Many studies have already been devoted to the analysis of the ro-vibrational spectra of methyl bromide in order to determine line positions and line intensities [32–36]. Concerning the determination of broadening coefficients, several efforts have been made by different groups either on CH_3Br self-broadened or perturbed by N_2, O_2 and air. Using a high-resolution Fourier transform spectrometer Jacquemart et al. [37] have measured line positions and intensities as well as self- and N_2-broadening coefficients of about 1200 lines belonging to the ν_6 band of both $CH_3^{79}Br$ and $CH_3^{81}Br$ isotopologues. The temperature dependence of broadening coefficients for 1400 lines in the same band was also studied by Jacquemart and Tran [38]. Always on the ν_6 band, theoretical calculations of self- and N_2-broadening coefficients were performed recently at room [39] and various temperatures [40]. Hoffman and Davies [41] have used a tunable diode laser absorption spectrometer to measure the room temperature pressure broadening coefficients of 174 rotational transitions in the ν_5 fundamental band of methyl bromide ($CH_3^{79}Br$ and $CH_3^{81}Br$) around 6.9 μm.

As a continuation of these projects aiming at studying the broadening parameters of CH_3Br for atmospheric applications, the present work deals with the determination of self- and N_2-broadening coefficients of both $CH_3^{79}Br$ and $CH_3^{81}Br$ isotopologues. The measurements were carried out for 948 ro-vibrational lines belonging to P, Q and R branches of the ν_2 band, around 7.7 μm. The experimental broadening coefficients were derived by analyzing twelve Fourier transform spectra recorded at the LISA facility in Créteil. They were measured using a mono-spectrum non-linear least squares fitting algorithm, already used in several previous works. The extensive measurements for self- and N_2-broadening coefficients have been obtained for large sets of J and K values, for which clear J and K dependences have been observed. Empirical polynomial expression has been used to model the rotational K dependence of the experimental widths.

The work is structured as follows: Section 2 describes the experimental details and data inversion procedure, the obtained results are presented in Section 3, in which a discussion concerning the J and K dependence of collisional parameters, as well as a detailed comparison with literature data are carried out. Conclusions and remarks are addressed in Section 4.

Table 1
FTS and SPAC configurations.

Source	SiC Globar
Detector	HgCdTe (MCT)
Beam splitter	KBr/Ge
Maximum optical path difference (d_{MOPD})	180, 300 or 450 cm
Resolution = $0.9/d_{MOPD}$	0.005, 0.003 or 0.002 cm^{-1}
Aperture diameter	1.15 mm
Collimator focal length	418 mm
Apodization function	Boxcar
Phase correction	Mertz
Phase resolution	0.5 cm^{-1}
Transfer optics mirror coatings	Gold
Cell windows	CsBr
Cell Mirror coatings	Gold
Pressure gauges	MKS-627 D Baratron (2, 10 and 100 Torr)

2. Experimental details and collisional half width measurements

2.1. Experimental details

Twelve absorption spectra of methyl bromide were recorded using the high-resolution Fourier transform spectrometer (FTS) Bruker IF125HR located at the LISA facility in Créteil. The instrument was equipped with a KBr/Ge beamsplitter. A silicon carbide Globar source and a liquid nitrogen cooled HgCdTe (MCT) detector were used in conjunction with an optical filter, with a bandpass of 1150–1550 cm^{-1}, to minimize the size of the interferogram data files and also to improve the S/N ratio. The entire optical path was evacuated in order to minimize H_2O and CO_2 absorption. The aperture diameter (1.15 mm) of the spectrometer was set to maximize the intensity of IR radiation falling on the MCT detector without saturation or loss of spectral resolution. Spectra were recorded with a 40 kHz scanner frequency and a maximum optical path difference (d_{MOPD}) of 180, 300 or 450 cm. According to the Bruker definition (Resolution = $0.9/d_{MOPD}$), this corresponds to a resolution of 0.005, 0.003 or 0.002 cm^{-1}.

A short-path absorption cell (SPAC) made of Pyrex glass and equipped with CsBr windows was used for all the measurements. The SPAC is a White-type multipass cell with a base length of 0.20 m. In this experiment an optical path of 0.849(2) m was used. The N_2 (99.99% stated purity) and CH_3Br (99% stated purity with bromine at natural abundance i.e., 50.54% ^{79}Br and 49.46% ^{81}Br)

Table 2
Summary of experimental conditions used to record the Fourier transform infrared spectra of CH_3Br and CH_3Br-N_2.[a]

	CH_3Br–CH_3Br		CH_3Br–N_2		
#	CH_3Br pressure (Torr)	R (cm^{-1})/No. of scans	CH_3Br pressure (Torr)	N_2 pressure (Torr)	R (cm^{-1})/No. of scans
1	3.087(15)	0.002/392	2.0014(10)	3.027(15)	0.003/260
2	3.626(18)	0.002/392	2.501(13)	5.737(29)	0.003/268
3	4.511(23)	0.002/396	3.006(15)	6.996(35)	0.003/268
4	5.625(28)	0.002/420	6.233(31)	44.11(22)	0.005/260
5	2.490(12)	0.002/444	2.060(10)	15.08(8)	0.005/256
6	2.046(10)	0.002/448	2.506(13)	30.24(15)	0.005/246
7	1.499(7)	0.002/444	3.160(16)	50.30(25)	0.005/260
8	1.003(5)	0.002/444	5.553(28)	71.32(36)	0.005/264
9	0.6160(31)	0.002/460	10.06(5)	89.02(45)	0.005/268
10	0.2034(10)	0.002/452	2.219(11)	22.23(11)	0.005/264
11	6.205(31)	0.002/444	2.717(14)	40.18(20)	0.005/260
12	6.811(34)	0.002/456	5.006(25)	60.07(30)	0.005/260

All spectra are recorded with a path length of 0.849 (2) m at stabilized room temperature of 295 ± 1 K. The path length value takes into account the distance between the surface of the field mirror and the windows of the cell (2 × 2.45 cm). R is the spectral resolution (equal to 0.9 divided by the maximum optical path difference, d_{MOPD}).

[a] The absolute uncertainty on the pressure is equal to 0.5% of the given value.

samples were purchased from Sigma Aldrich. No further sample purifications were done.

The following procedure was used for measurements: first a background spectrum was collected while the cell was being continuously evacuated. Next, the cell was filled with CH_3Br at a given pressure. Finally, the perturber gas was added in stages leading to a series of 12 pressures. One CH_3Br/N_2 spectrum is recorded for each CH_3Br fill. The sample pressure in the cell was measured using calibrated MKS Baratron capacitance manometers (2, 10 or 100 Torr full scale) with a reading accuracy of 0.12%, according to the manufacturer. To estimate the uncertainty of the sample pressure, we add the uncertainty arising from the small variation of the pressure during the recording (~0.35%) and the accuracy of the gauge; this leads to an estimation of 0.5% uncertainty on the pressure.

The spectra were recorded at a stabilized room temperature of 295 ± 1 K. All spectra were ratioed against a single channel background spectrum of the empty cell which was recorded at a resolution of 0.2 cm^{-1} in order to ensure the best possible signal-to-noise in the ratioed spectra. For the Fourier transform, a Mertz-phase correction, 0.5 cm^{-1} phase resolution, a zero-filling factor of 2 and a boxcar apodization function were applied to the averaged interferograms. The FTS instrumental parameters and settings are summarized in Table 1. Details of the pressures and the number of scans taken for each sample are given in Table 2. The Signal/Noise ratio (RMS) in our spectra are between 139 and 226 (for self spectra) and between 344 and 560 for CH_3Br/N_2 spectra.

2.2. Collisional half width measurements

The collisional half widths were measured using a mono-spectrum non-linear least squares fitting algorithm, already used and described in previous works [36,42–44]. In brief, the measurements involved the adjustment of a calculated spectrum to the observed spectrum using a Levenberg–Marquardt non-linear least squares fitting procedure [45]. Each calculated spectrum was computed as the convolution of a monochromatic transmission spectrum with an instrument line shape function, which includes the effects of the finite maximum optical path difference and of the finite source aperture diameter of the interferometer [46].

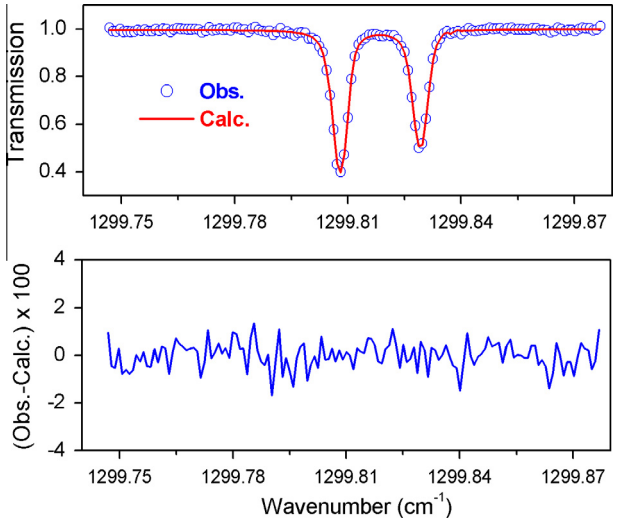

Fig. 1. Part of the P-branch ((P_{79}(11, E, 7) and P_{79}(12, A^+, 9) lines) of the ν_2 band of CH_3Br self-perturbed (open circles in the upper panel), and the best fit calculated spectrum (solid line) obtained with a source aperture diameter of 1.15 mm, a maximum optical path difference of 450 cm and a Voigt profile. The observed spectrum is recorded at a CH_3Br pressure of 3.087 Torr, at 0.002 cm^{-1} resolution using 392 scans. The lower panel is a residual plot showing percent differences between the observed and calculated spectra.

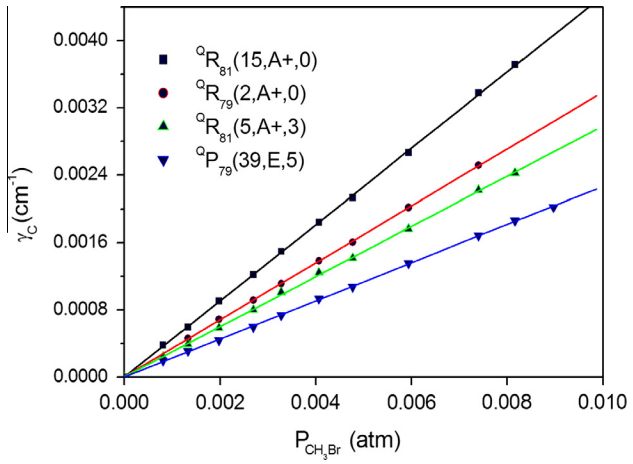

Fig. 2. Pressure dependence of the collisional half width $\gamma_c = \gamma_{self} P_{CH_3Br}$ for the $^{Q}R_{81}$(15, A+, 0), $^{Q}R_{79}$(2, A+, 0), $^{Q}R_{81}$(5, A+, 3) and $^{Q}P_{79}$(39, E, 5) lines in the ν_2 band of CH_3Br. The slopes of the best-fit lines represent the self-broadening coefficients. No weighted values are used for these lines.

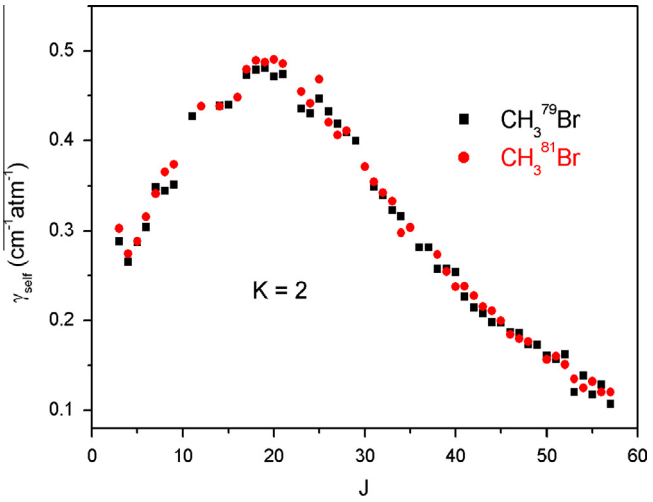

Fig. 3. *J*-dependence of the measured self-broadening coefficients in the P-branch of $CH_3^{79}Br$ and $CH_3^{81}Br$ with $K = 2$.

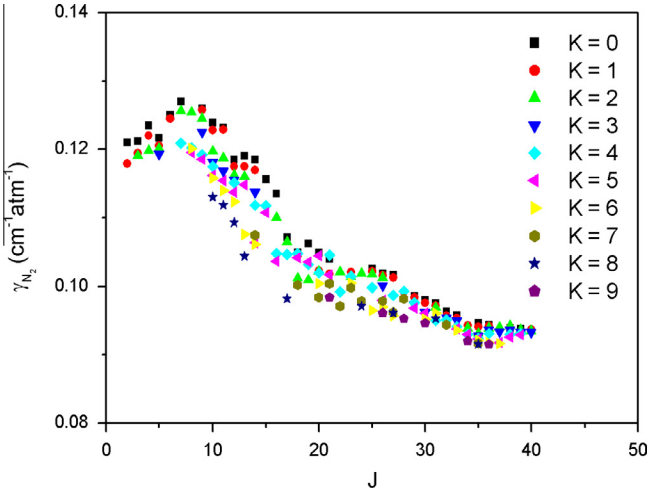

Fig. 4. *J*-dependence of the measured N_2-broadening coefficients in the R-branch of $CH_3^{79}Br$ for *K* ranging from 0 to 9.

The line profile was modeled using a Voigt function, with Gaussian width always held fixed to the value calculated for the Doppler broadening, without introducing line mixing. In addition, for the background, a slope and a curvature can also be varied. An example of the quality of the fitting procedure is given in Fig. 1. The upper panel shows the observed and calculated spectra overlaid; the lower panel gives the difference between the two in percent. As it can be seen, the Voigt profile reproduces satisfactorily the experimental features: the small residuals suggest that the Voigt profile is well suited to fit the experimental line shapes. At this point, it should be mentioned that the narrowing effects are negligible, i.e., the typical residuals are not observed. Indeed, when the mean free path of a molecule is much smaller than the wavelength of the radiative transition, the molecule changes velocity and direction many times during the emission or absorption of a photon. This causes an averaging over different Doppler states and results in a molecular linewidth that is narrower than the Doppler width. This effect, also known as Dicke narrowing [47], is very small (about ±1%) [48] and is not easily observable by Fourier transform spectroscopy. In our case this effect is probably hidden in noise and is neglected in this work, as mentioned by Bray et al. [49], it is greatly masked by the large collisional broadenings of N_2 and CH_3Br with a large dipole moment.

The self- and N_2-broadening coefficients, γ_{self} and γ_{N2}, for the rovibrational lines measured in the present study, were derived by a linear fit of the collisional half widths, as retrieved from the line profile analysis, against the pressure of the perturbing species, CH_3Br or N_2:

$$\gamma_c = \gamma_{self} P_{CH_3Br} + \gamma_{N_2} P_{N_2} \quad (1)$$

where γ_c is the collisional half width, P_{CH_3Br} and P_{N_2} are respectively CH_3Br and N_2 partial pressure. A typical plot of the collisional half widths γ_c derived from the fittings versus the CH_3Br pressures, is shown in Fig. 2 for the $^{Q}R_{81}$(15, A+, 0), $^{Q}R_{79}$(2, A+, 0), $^{Q}R_{81}$(5, A+, 3) and $^{Q}P_{79}$(39, E, 5) lines in the ν_2 band of CH_3Br. The straight lines obtained from the fitting show a good verification of the linearity of the collisional half widths against pressure. The self- and N_2-broadening coefficients (in cm^{-1} atm^{-1}) can be derived from the slopes of these straight lines. A total of 948 broadening coefficients were obtained and collected in the third and fifth column of Supplementary material include to this paper.

The precision of the measurements (2σ) can be judged by examining the residuals of the fits. They are generally less than 2%. However, a better estimation of the accuracy of the broadening coefficients requires taking into consideration the uncertainties on the physical parameters, the purity of the sample and contributions from possible systematic errors [50]. The dominant contributions to the systematic errors were found to arise from offsets in the 0% transmission level and nonlinearities in the response of the MCT detector. We estimate that the accuracy of the broadening coefficients measured in this work is between 4% and 8%, depending on the studied transition.

3. Results and discussion

The self- and N_2-broadening coefficients for CH_3Br transitions in the ν_2 band retrieved from our mono-spectrum analysis are presented in Supplementary material include to this paper. The assignment column gives the isotopologue (79 for $CH_3^{79}Br$ and 81 for $CH_3^{81}Br$) for which the transition is observed, the type of branch, the rotational quantum number J of the lower state, its symmetry, and the rotational quantum number K of the lower state. Position column corresponds to line positions in cm^{-1}. γ_{self} and γ_{N2} are the measured self- and N_2-broadening coefficients in cm^{-1} atm^{-1}. %self and $\%N_2$ are the differences in % between the experimental and calculated widths. The calculated values are obtained using a polynomial empirical fit of the measured ones (see Section 3.2). In our analysis, we have not applied any temperature corrections to the measured broadening coefficients. Hence, the broadening coefficients listed in Supplementary material correspond to values at 295 ± 1 K at which the spectra were recorded. We present our results arranged in groups of P, Q and R branches. The precision of the measurements given in Supplementary material represents two standard deviation uncertainties in the measured quantities in units of the last quoted digit.

3.1. Discussion of the measured self- and N_2-broadening coefficients

Extensive measurements of self- and N_2-broadening coefficients have been obtained for a large number of J and K values ranging from 2 to 49 and from 0 to 10, respectively. The measured self-broadening coefficients range from 0.1542 to 0.4930 cm^{-1} atm^{-1};

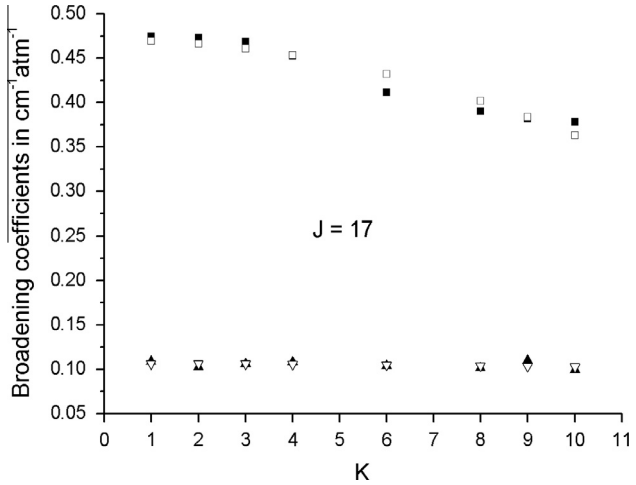

Fig. 5. Example of the polynomial fit in K (using Eq. (3)) of the self- and N_2-broadening coefficients with $J = 17$ for $CH_3^{79}Br$. The black triangles (▲) and squares (■) symbols represent, respectively, the measured N_2- and self-broadening coefficients, whereas the open triangles (▽) and squares (□) have been used to reproduce, respectively, the calculated N_2- and self-broadening coefficients.

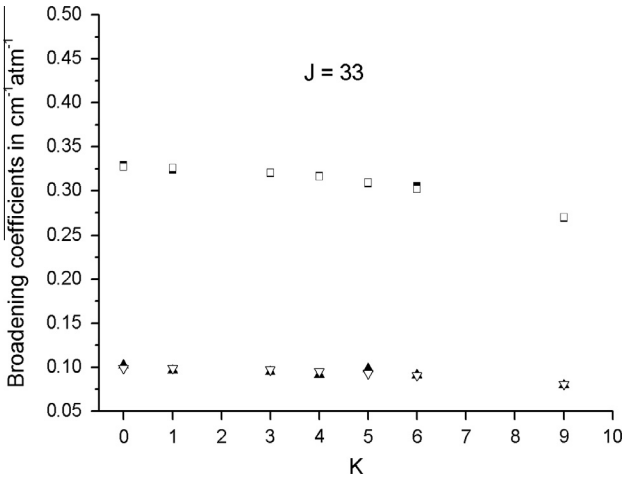

Fig. 6. Example of the polynomial fit in K (using Eq. (3)) of the self- and N_2-broadening coefficients with $J = 33$ for $CH_3^{79}Br$. The black triangles (▲) and squares (■) symbols represent, respectively, the measured N_2- and self-broadening coefficients, whereas the open triangles (▽) and squares (□) have been used to reproduce, respectively, the calculated N_2- and self-broadening coefficients.

Table 3
Best-fit coefficients a_J^0 and a_J^2 (in $cm^{-1}\,atm^{-1}$) of Eq. (3) used to reproduce the measured self- and N_2-broadening parameters of the ν_2 band of $CH_3^{79}Br$.

J	Self		N_2	
	a_J^0	a_J^0	a_J^2	a_J^0
P branch				
5	0.3127(16)	−0.00333(33)	0.1227(6)	−0.000340(12)
7	0.3595(91)	−0.00483(11)	0.1216(16)	−0.000464(20)
8	0.3554(39)	−0.00234(24)	0.1266(2)	−0.000324(13)
9	0.3779(95)	−0.00231(53)	0.1265(1)	−0.000280(6)
11	0.4303(38)	−0.00194(15)	0.1229(15)	−0.000200(58)
12	0.4322(29)	−0.00156(8)	0.1213(13)	−0.000222(34)
14	0.4430(25)	−0.00120(7)	0.1180(12)	−0.000229(33)
15	0.4462(25)	−0.00112(6)	0.1158(20)	−0.000203(48)
16	0.4513(34)	−0.000789(59)	0.1154(19)	−0.000172(33)
17	0.4706(64)	−0.00108(12)	0.1064(20)	−0.0000378(37)
18	0.4898(48)	−0.00126(12)	0.1062(18)	−0.0000801(46)
20	0.4972(35)	−0.00154(15)	0.1079(22)	−0.000267(95)
21	0.4792(43)	−0.00114(15)	0.1086(13)	−0.0000881(49)
22	0.4784(62)	−0.00127(18)	0.1103(23)	−0.000273(64)
23	0.4506(56)	−0.000747(13)	0.1059(31)	−0.000141(69)
24	0.4516(65)	−0.000684(13)	0.1059(16)	−0.000149(37)
25	0.4541(21)	−0.00112(5)	0.1033(23)	−0.0000913(57)
26	0.4372(91)	−0.000880(24)	0.1007(19)	−0.0000649(49)
27	0.3995(13)	−0.000498(26)	0.0989(18)	−0.00000334(38)
28	0.4255(74)	−0.00178(42)	0.0984(23)	−0.0000652(103)
29	0.3992(16)	−0.00146(11)	0.1029(10)	−0.000330(71)
30	0.3693(25)	−0.000430(13)	0.1002(30)	−0.000246(15)
31	0.3481(9)	−0.000168(46)	0.0976(31)	−0.0000221(16)
32	0.3413(41)	−0.000725(100)	0.1007(20)	−0.000224(48)
33	0.3271(13)	−0.000702(37)	0.0990(18)	−0.000227(50)
34	0.3240(78)	−0.000616(30)	0.1002(17)	−0.000311(67)
35	0.3167(99)	−0.000255(28)	0.0975(18)	−0.000172(53)
36	0.2847(70)	−0.000357(17)	0.0974(23)	−0.000123(55)
37	0.2800(63)	−0.000526(18)	0.0966(22)	−0.000167(63)
38	0.2653(23)	−0.000553(18)	0.0982(37)	−0.000379(29)
39	0.2616(25)	−0.000717(80)	0.0924(24)	−0.000197(75)
42	0.2309(107)	−0.00135(12)	0.0975(6)	−0.000281(70)
43	0.2194(45)	−0.00130(55)	0.0952(38)	−0.0000892(47)
44	0.2099(42)	−0.000446(16)	0.0927(9)	−0.000214(32)
45	0.1952(38)	−0.000323(19)	0.0906(24)	−0.000123(13)
Q branch				
8	0.3137(145)	−0.00167(34)	0.1208(18)	−0.0000638(42)
9	0.3082(138)	−0.00101(26)	0.1240(13)	−0.0000979(240)
10	0.3401(70)	−0.00142(10)	0.1217(49)	−0.000178(73)
12	0.3410(223)	−0.000839(30)	0.1137(25)	−0.000103(34)
R branch				
5	0.3196(50)	−0.00279(10)	0.1212(4)	−0.000224(74)
8	0.2799(32)	−0.000027(14)	0.1246(20)	−0.000162(86)
9	0.3912(25)	−0.00217(20)	0.1257(5)	0.000327(39)
10	0.3896(33)	−0.00109(12)	0.1212(9)	−0.000148(31)
11	0.4065(69)	−0.000976(23)	0.1207(11)	−0.000162(37)
12	0.4159(58)	−0.00131(21)	0.1173(3)	−0.000132(11)
13	0.4133(63)	−0.00121(20)	0.1180(10)	−0.000221(33)
14	0.4142(62)	−0.000954(24)	0.1164(15)	−0.000246(57)
16	0.4482(34)	−0.000804(23)	0.1123(12)	−0.000386(79)
17	0.4526(27)	−0.00138(8)	0.1071(1)	−0.000139(3)
18	0.4464(32)	−0.000962(87)	0.1049(11)	−0.000118(28)
19	0.4564(60)	−0.00174(40)	0.1039(20)	−0.0000325(14)
20	0.4507(57)	−0.000976(153)	0.1045(10)	−0.000142(28)
21	0.4411(12)	−0.000969(30)	0.1036(8)	−0.0000620(193)
23	0.4190(12)	−0.000778(41)	0.1021(2)	−0.0000466(56)
25	0.3976(43)	−0.000733(99)	0.1025(1)	−0.000166(3)
26	0.3862(20)	−0.000500(54)	0.1011(5)	−0.0000721(133)
27	0.3863(17)	−0.000940(47)	0.1009(8)	−0.0000940(211)
28	0.3632(22)	−0.000626(46)	0.0998(6)	−0.0000490(131)
29	0.3686(14)	−0.00115(10)	0.0984(2)	−0.0000656(166)
30	0.3429(40)	−0.000700(105)	0.0972(4)	−0.0000381(100)
31	0.3283(42)	−0.000458(14)	0.0968(5)	−0.0000304(59)
32	0.3257(37)	−0.000561(14)	0.0958(2)	−0.0000323(63)
33	0.3221(16)	−0.000807(81)	0.0955(2)	−0.0000612(99)
34	0.2988(57)	−0.000253(11)	0.0937(4)	−0.0000102(25)
35	0.2973(31)	−0.000760(117)	0.0937(3)	−0.0000484(118)
36	0.2831(19)	−0.000602(47)	0.0940(2)	−0.0000369(57)
37	0.2548(10)	−0.000204(45)	0.0941(3)	−0.0000780(140)
38	0.2540(36)	−0.000812(28)	0.0941(1)	−0.0000612(97)
39	0.2456(42)	−0.000926(30)	0.0937(1)	−0.0000359(45)

Note: Numbers between parentheses are the uncertainties (1σ) in the units of the last quoted digit.

and the N_2-broadening coefficients range from 0.0737 to 0.1284 $cm^{-1}\,atm^{-1}$. Fig. 3 is a plot of the J-dependence of the measured self-broadening coefficients in the P-branch of $CH_3^{79}Br$ and $CH_3^{81}Br$ with $K = 2$. This figure shows that for a given K, the self-broadening coefficients tend to increase until reaching a maximum, at 0.4930 $cm^{-1}\,atm^{-1}$ for $J_{max} = 20$ ($K = 0$) for the $CH_3^{79}Br$ isotope and 0.4909 $cm^{-1}\,atm^{-1}$ for $J_{max} = 20$ ($K = 2$) for the $CH_3^{81}Br$ isotope, then started to decrease for higher J. Note that no significant discrepancy has been observed between the measurement of self-broadening coefficients of $CH_3^{79}Br$ and $CH_3^{81}Br$.

The position of the maximum self-broadening coefficients is corresponding to the maximum of efficiency for collision dominated by the electrostatic interactions. This maximum value J_{max} is given by the resonance condition [51,52]:

$$J_{max} \approx \frac{B_2\, l_2}{B_1\, l_1} J_{2p} \tag{2}$$

J_{2P} is the most populated level of the perturbing molecule at the temperature considered (for CH_3Br at room temperature $J_{2p} \approx 17$). B_1 and B_2 are the rotational constants of the two partners ($B_1 = B_2$ for CH_3Br self-perturbed). The spherical harmonic orders l_i depend on the nature of the interaction. Therefore for the self broadening dominated by the dipole–dipole interaction ($l_1 = l_2 = 1$), the maximum collision effectiveness is around $J_{max} = J_{2p}$ in overall agreement with the experimental observation.

In Fig. 4, we have plotted the J-dependence of the measured N_2-broadening coefficients in the R-branch of $CH_3^{79}Br$ for K ranging from 0 to 9. It is found that this variation has a maximum at $J_{max} = 7$. For N_2 at room temperature $J_{2P} \approx 7$. The rotational constants are $B_1 = 0.3185542$ [53] and $B_2 = 1.989622$ [54].

If one considers that the N_2 broadenings are dominated by the dipole-quadrupole interaction, the spherical harmonic orders are $l_1 = 1$ and $l_2 = 2$, and the maximum of collision effectiveness will be at $J_{max} \approx 44$, in disagreement with the experimental observation ($J_{max} = 7$ for $CH_3^{79}Br$). In this case Eq. (2) is unable to predict the J_{max} value CH_3Br–N_2 system proving that the dipole–quadripole interaction is not the main contribution of this collision.

3.2. Empirical polynomial expression to describe the broadening coefficients in term of K

We have fitted the experimental self- and N_2-broadening coefficients to an empirical polynomial expression as previously done in Refs. [55–58]. Such a work requires a great amount of accurate measurements. For methyl bromide, the study of Jacquemart et al. [37] on the ν_6 band can be cited as recent work dealing with the rotational dependence of broadening coefficients for large sets of J and K values. In order to correctly model the line widths, we chose to fit the broadening coefficients by a polynomial expression for each value of J as a function of K:

$$\gamma_J(K) = a_J^0 + a_J^2 K^2 \tag{3}$$

Table 4
Best-fit coefficients a_J^0 and a_J^2 (in $cm^{-1}atm^{-1}$) of Eq. (3) used to reproduce the measured self- and N_2-broadening parameters of the ν_2 band of $CH_3^{81}Br$.

J	Self		N_2	
	a_J^0	a_J^2	a_J^0	a_J^2
P branch				
5	0.3218(16)	−0.00630(108)	0.1237(10)	−0.000432(20)
6	0.3512(40)	−0.00299(44)	0.1220(7)	−0.000255(74)
7	0.3593(59)	−0.00350(42)	0.1191(3)	−0.000220(25)
8	0.3792(54)	−0.00384(65)	0.1272(6)	−0.000360(73)
9	0.3866(32)	−0.00238(16)	0.1265(4)	−0.000234(22)
14	0.4448(94)	−0.00140(24)	0.1189(16)	−0.000242(40)
15	0.4367(12)	−0.00110(27)	0.1156(24)	−0.000156(55)
16	0.4564(53)	−0.00130(14)	0.1149(18)	−0.000214(48)
17	0.4861(15)	−0.00166(17)	0.1096(30)	−0.0000965(314)
18	0.4960(24)	−0.00123(8)	0.1089(8)	−0.000189(30)
19	0.4927(68)	−0.00109(24)	0.1090(30)	−0.000202(11)
20	0.5016(64)	−0.00139(17)	0.1088(23)	−0.000262(63)
21	0.4870(42)	−0.00108(10)	0.1065(22)	−0.0000928(49)
22	0.4779(47)	−0.000961(123)	0.1032(27)	−0.0000988(65)
23	0.4645(51)	−0.000833(119)	0.1086(29)	−0.000180(33)
24	0.4409(37)	−0.000415(90)	0.1057(23)	−0.000105(27)
25	0.4333(48)	−0.000744(119)	0.1025(7)	−0.0000753(168)
26	0.4216(49)	−0.000763(149)	0.1038(9)	−0.000100(28)
27	0.4149(50)	−0.000794(141)	0.1012(14)	−0.0000878(204)
28	0.4204(45)	0.00110(267)	0.1004(16)	−0.000124(9)
29	0.4042(26)	−0.00155(11)	0.0984(43)	−0.0000643(183)
30	0.3720(11)	−0.000358(29)	0.1001(31)	−0.000160(41)
31	0.3597(25)	−0.000444(102)	0.1065(17)	−0.000380(67)
32	0.3420(12)	−0.000128(35)	0.0975(23)	−0.000133(32)
33	0.3336(32)	−0.00118(17)	0.0990(27)	−0.000300(71)
34	0.2935(23)	−0.000343(64)	0.1032(22)	−0.000210(61)
35	0.3035(55)	−0.000143(14)	0.0936(7)	−0.000110(14)
36	0.3028(39)	−0.00117(26)	0.0924(2)	−0.0000464(150)
37	0.3015(33)	−0.00175(24)	0.0984(13)	−0.000284(91)
38	0.2690(50)	−0.000617(146)	0.0939(23)	−0.000129(34)
39	0.2612(30)	−0.000511(106)	0.0955(15)	−0.000161(52)
44	0.2101(58)	−0.000315(29)	0.0908(21)	−0.000214(52)
45	0.2028(14)	−0.000437(54)	0.0878(23)	−0.0000607(89)
46	0.1891(11)	−0.000468(43)	0.0913(36)	−0.000109(14)
Q branch				
8	0.3336(15)	−0.00182(38)	0.1225(22)	−0.000104(26)
9	0.3294(16)	−0.00125(24)	0.1247(21)	−0.000148(32)
10	0.3485(75)	−0.00149(12)	0.1216(29)	−0.000171(48)
R branch				
5	0.3255(54)	−0.00346(109)	0.1218(1)	−0.000324(15)
6	0.3025(88)	−0.00197(58)	0.1253(1)	−0.000504(13)
7	0.2974(8)	−0.000634(37)	0.1257(3)	−0.000221(16)
8	0.3005(30)	−0.000608(153)	0.1259(14)	−0.000183(35)
9	0.3956(26)	−0.00227(15)	0.1256(8)	−0.000238(45)
10	0.3982(20)	−0.00137(8)	0.1228(12)	−0.000195(51)
11	0.4052(29)	−0.00108(12)	0.1209(11)	−0.000184(46)
12	0.4149(28)	−0.00160(16)	0.1181(8)	−0.000170(46)
13	0.4126(50)	−0.00127(19)	0.1187(7)	−0.000230(29)
14	0.4275(32)	−0.00104(10)	0.1166(10)	−0.000214(29)
15	0.4469(40)	−0.00119(11)	0.1155(2)	−0.000186(7)
16	0.4554(44)	0.00117(11)	0.1107(12)	−0.000162(30)
17	0.4540(12)	−0.00174(9)	0.1062(15)	−0.000104(10)
18	0.4551(56)	−0.000836(142)	0.1035(10)	−0.0000331(25)
19	0.4610(60)	−0.00118(24)	0.1045(18)	−0.000164(36)
20	0.4635(58)	−0.00158(26)	0.1043(17)	−0.0000656(79)
21	0.4429(10)	−0.000961(115)	0.1033(7)	−0.0000595(109)
22	0.4397(75)	−0.00117(23)	0.1022(6)	−0.000106(19)
23	0.4229(57)	−0.000983(205)	0.1027(2)	−0.0000590(65)
24	0.3955(50)	−0.000379(101)	0.1036(11)	−0.000126(21)
25	0.3960(31)	−0.000742(92)	0.1025(2)	−0.000126(7)
26	0.3936(6)	−0.000493(17)	0.1012(6)	−0.0000641(155)
27	0.3860(26)	−0.000774(82)	0.1010(4)	−0.0000628(128)
28	0.3695(28)	−0.000496(65)	0.0996(2)	−0.0000227(53)
29	0.3631(37)	−0.000728(124)	0.0986(2)	−0.0000594(80)
30	0.3495(59)	−0.000749(152)	0.0981(3)	−0.0000507(89)
31	0.3293(47)	−0.000343(75)	0.0974(1)	−0.0000246(40)
32	0.3232(37)	−0.000405(89)	0.0966(2)	−0.0000324(45)
33	0.3027(85)	−0.000297(54)	0.0962(1)	−0.0000888(41)
34	0.3149(30)	−0.000704(117)	0.0952(2)	−0.0000664(97)
35	0.3084(46)	−0.000986(253)	0.0949(2)	−0.0000886(131)
36	0.2841(47)	−0.000543(125)	0.0944(2)	−0.0000358(64)
37	0.2660(35)	−0.000507(101)	0.0942(3)	−0.0000469(75)
39	0.2358(14)	−0.000141(26)	0.0934(4)	−0.0000287(75)
40	0.2407(66)	−0.000898(164)	0.0940(1)	−0.0000450(47)

Note: Numbers between parentheses are the uncertainties (1σ) in the units of the last quoted digit.

Examples of these fits are given in Figs. 5 and 6 for transitions with $J = 17$ and 33 respectively, for $CH_3^{79}Br$. As it has been observed in numerous works concerning C_{3v} molecules [37,55–58], the broadening coefficients decrease with K. This decrease is more significant at low J than at high J values.

The best-fit coefficients a_J^0 and a_J^2 were determined through a least-squares fit of the experimental broadening coefficients. These coefficients are listed in Tables 3 and 4 for $CH_3^{79}Br$ and $CH_3^{81}Br$, respectively. The discrepancies between experimental and calculated broadening coefficients are presented in column named %self and $\%N_2$ of Supplementary material. A statistical analysis (Table 5) of the calculated values (γ_{emp}) shows that the fit is very good since 98% of the broadening coefficients fall within 6% of the observed values (γ_{obs}). This latter range corresponds to the measurement uncertainty for the broadening coefficients.

3.3. Comparison with previous measurements in the ν_5 and ν_6 bands

We focus our interest on the m ($m = -J, J$ and $J + 1$ for P-, Q- and R-branch lines) quantum number dependence of the CH_3Br broadening coefficients and how the present determinations compare to the literature ones. Indeed, the datasets of the molecules in the databases are continuously revised by the inclusion of recent results. Sometimes, due to the absence of the necessary information, the spectroscopic parameters obtained for a given vibrational band are attributed to the corresponding lines of another band. On the other hand, many authors have discussed the vibrational dependence of broadening coefficients. In most cases, the comparison exhibits no or small vibrational dependence.

In this work for the ν_2 parallel band, although no appropriate, the comparison is made with the works of Jacquemart et al. [37] and Hoffman and Davies [41] in the ν_6 and ν_5 perpendicular bands respectively. These data are the only available in the literature. The self-broadening coefficients are plotted in Fig. 7 which shows a comparison between the present results of the R-branch in the ν_2 parallel band and the previous measurements of the ^RQ-branch in ν_5 [41] and ν_6 [37] perpendicular bands. The values of the ν_5 band appear larger than our results (the average percentage difference is about 13%) or those of the ν_6 band (the average percentage difference is about 12%). Our results are in satisfactory agreement with those of the ν_6 band because the average difference is about 7.8% for $CH_3^{79}Br$ and 4% for $CH_3^{81}Br$.

Concerning the N_2-broadening coefficients, it is evident from Fig. 8 that our values and those of the ν_6 band are slightly greater than the data obtained in the ν_5 band. The average percentage difference between our values and those of the ν_6 band is about 1.2% for $CH_3^{79}Br$ and 2% for $CH_3^{81}Br$; and about 5% with those of the ν_5 band.

Finally, the broadening coefficients obtained by Jacquemart et al. [37] in the ν_6 band are in overall good agreement with the present values. On the other side we observe systematic differences between the present measurements in ν_2 and the previous ones in ν_5 [41], as shown in Figs. 7 and 8.

Table 5
Statistical analysis of the fit results for the experimental and empirical broadening coefficients of CH_3Br self- and N_2-perturbed.

	CH_3Br broadener gas		N_2 broadener gas	
	$CH_3^{79}Br$	$CH_3^{81}Br$	$CH_3^{79}Br$	$CH_3^{81}Br$
Number of lines used in the fit	408	425	406	422
J_{max}	45	46	45	46
K_{max}	10	10	10	10
$0\% \leqslant \delta < 3\%$	81%	85%	83%	89%
$3\% \leqslant \delta < 7\%$	17%	14%	16%	9%
$7\% \leqslant \delta < 9\%$	2%	1%	1%	2%

$\delta = |\gamma_{obs} - \gamma_{emp}|/\gamma_{obs} \times 100$.

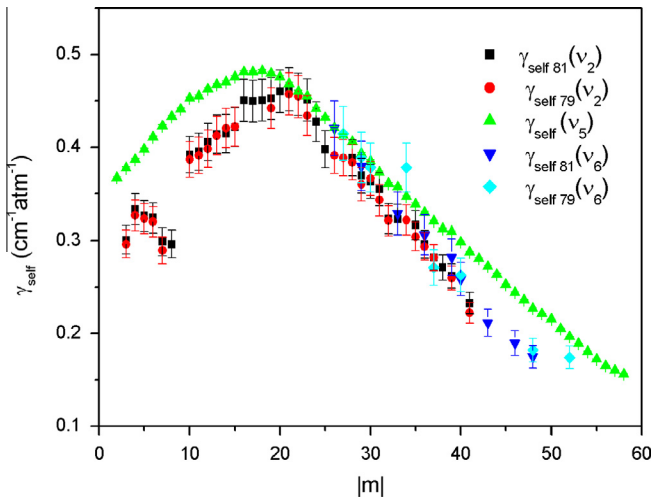

Fig. 7. m-dependence of self-broadening coefficients measured in the ν_2 band of CH_3Br in this work and comparison to literature values in the ν_5 [37] and ν_6 [41] bands of CH_3Br. $m = -J$, J and $J+1$ for P-, Q- and R-branch lines. The error bars indicate the estimated accuracies of the measurements.

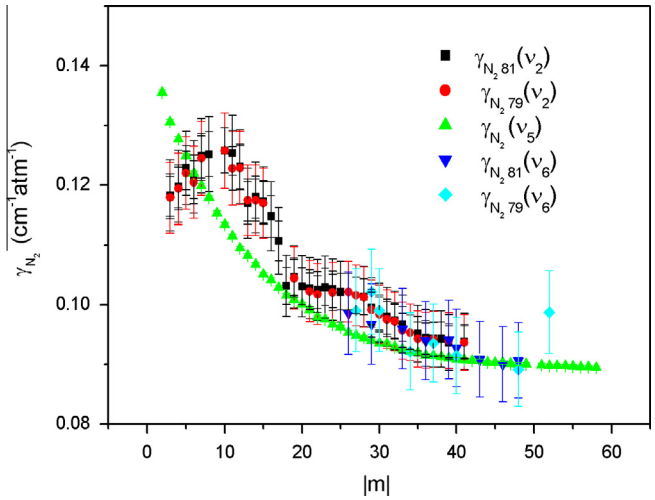

Fig. 8. m-dependence of N_2-broadening coefficients measured in the ν_2 band of CH_3Br in this work and comparison to literature values in the ν_5 [37] and ν_6 [41] bands of CH_3Br. $m = -J$, J and $J+1$ for P-, Q- and R-branch lines. The error bars indicate the estimated accuracies of the measurements.

4. Conclusions

Twelve high-resolution spectra on the ν_2 band of methyl bromide have been recorded and analyzed with a mono-spectrum non-linear least squares fitting technique. It results in the determination of the self- and N_2-broadening coefficients for 948 ν_2 band lines of CH_3Br, up to $J = 49$ and $K = 10$. A Voigt function appeared to properly model the observed molecular line shapes within the noise level and a total of 948 broadening coefficients have been measured. The accuracy of these measurements is between 4% and 8%, depending on the studied transition. These broadening coefficients have been obtained for large sets of J and K values, for which clear J and K dependences have been observed.

Empirical polynomial expression have been used to model the rotational K dependence of the broadening coefficients, leading to accurate coefficients constants (a_J^0 and a_J^2) for both $CH_3^{79}Br$ and $CH_3^{81}Br$ isotopologues. Comparisons with measurements taken in the ν_5 and ν_6 bands of CH_3Br did not show any clear vibrational dependence. Indeed, the broadening coefficients obtained in the ν_6 band are in overall good agreement with the present values. On the other side we observe systematic differences between the present measurements in ν_2 and the previous ones in ν_5 illustrating a small vibrational effect.

To summarize, the present results represent a complete and systematic investigation of the broadening parameters of methyl bromide in the ν_2 band, which are of relevance for atmospheric remote sensing applications.

Appendix A. Supplementary material

Supplementary data associated with this article can be found, in the online version, at http://dx.doi.org/10.1016/j.jms.2014.12.018.

References

[1] G. Duxbury, Infrared Vibration-Rotation Spectroscopy. From Free Radicals to the Infrared Sky, John Wiley & Sons, Chichester, 2000.
[2] J. Demaison, K. Sarka, E.A. Cohen, Spectroscopy from Space, NATO Science Series, Kluwer Academic Publisher, London, 2001.
[3] F. Niro, F. Hase, C. Camy-Peyret, S. Payan, J.M. Hartmann, J. Quant. Spectrosc. Radiat. Transfer 90 (2005) 43–59.
[4] K.G. Hay, S. Wright, G. Duxbury, N. Langford, Appl. Phys. B 90 (2008) 329–337.
[5] G. Duxbury, N. Langford, K. Hay, N. Tasinato, J. Mod. Opt. 56 (2009) 2034–2048.
[6] D. McNaughton, E.G. Robertson, D. Thompson, T. Chimdi, M.K. Bane, D. Appadoo, J. Anal. Chem. 82 (2010) 7958–7964.
[7] A.T. Brown, M.P. Chipperfield, C. Boone, C. Wilson, K.A. Walker, P.F. Bernath, J. Quant. Spectrosc. Radiat. Transfer 112 (2011) 2552–2566.
[8] M.R. Swain, G. Vasisht, G. Tinetti, Nature 452 (2008) 329–331.
[9] G. Tinetti, A. Vidal-Madjar, M.-C. Liang, J.-P. Beaulieu, Y. Yung, S. Carey, R.J. Barber, J. Tennyson, I. Ribas, N. Allard, G.E. Bellester, D.K. Sing, F. Selsis, Nature 448 (2007) 169–171.
[10] M. Lepère, Spectrochim. Acta A 60 (2004) 3249–3258.
[11] J. Walrand, M. Lengelé, G. Blanquet, Spectrochim. Acta A 60 (2004) 3299–3303.
[12] L.R. Brown, D.C. Benner, V. Malathy Devi, M.A.H. Smith, R.A. Toth, J. Mol. Struct. 742 (2005) 111–122.
[13] J. Orphal, J.-M. Flaud, Q. Kou, F. Kwabia Tchana, O. Pirali, J. Mol. Struct. 742 (2005) 153–159.
[14] C.N. Harward Sr., W.D. Thweatt, R.E. Baren, M.P. Parrish, Spectrochim. Acta A 63 (2006) 970–980.
[15] M.A. Koshelev, M. Yu Tretyakov, R.M. Lees, L.-H. Xu, J. Mol. Struct. 780–781 (2006) 7–16.
[16] J. Vander Auwera, A. Fayt, J. Mol. Struct. 780–781 (2006) 134–141.
[17] A.I. Nadezhdinskii, Ya.Ya. Panurovskii, Spectrochim. Acta A 66 (2007) 807–810.
[18] N. Tasinato, P. Stoppa, A. Pietropolli Charmet, S. Giorgianni, G. Buffa, A. Gambi, ChemPhysChem 12 (2011) 356–363.

[19] L.S. Rothman, I.E. Gordon, Y. Babikov, A. Barbe, D. Chris Benner, P.F. Bernath, M. Birk, L. Bizzocchi, V. Boudon, L.R. Brown, A. Campargue, K. Chance, E.A. Cohen, L. Coudert, V.M. Devi, B.J. Drouin, A. Fayt, J.-M. Flaud, R.R. Gamache, J.J. Harrison, J.-M. Hartmann, C. Hill, J.T. Hodges, D. Jacquemart, A. Jolly, J. Lamouroux, R.J. LeRoy, G. Li, D.A. Long, O.M. Lyulin, C.J. Mackie, S.T. Massie, S. Mikhailenko, H.S.P. Müller, O.V. Naumenko, A.V. Nikitin, J. Orphal, V. Perevalov, A. Perrin, E.R. Polovtseva, C. Richard, M.A.H. Smith, E. Starikova, K. Sung, S. Tashkun, J. Tennyson, G.C. Toon, Vl.G. Tyuterev, G. Wagner, J. Quant. Spectrosc. Radiat. Transfer 130 (2013) 4–50.
[20] N. Jacquinet-Husson, L. Crepeau, R. Armante, C. Boutammine, A. Chédin, N.A. Scott, C. Crevoisier, V. Capelle, C. Boone, N. Poulet-Crovisier, A. Barbe, A. Campargue, D. Chris Benner, Y. Benilan, B. Bézard, V. Boudon, L.R. Brown, L.H. Coudert, A. Coustenis, V. Dana, V.M. Devi, S. Fally, A. Fayt, J.-M. Flaud, A. Goldman, M. Herman, G.J.Harris, D. Jacquemart, A. Jolly, I. Kleiner, A. Kleinböhl, F. Kwabia Tchana, N. Lavrentieva, N. Lacome, Li-Hong Xu, O.M. Lyulin, J.-Y. Mandin, A. Maki, S. Mikhailenko, C.E. Miller, T. Mishina, N. Moazzen-Ahmadi, H.S.P. Müller, A. Nikitin, J. Orphal, V. Perevalov, A. Perrin, D.T. Petkie, A. Predoi-Cross, C.P. Rinsland, J.J. Remedios, M. Rotger, M.A.H. Smith, K. Sung, S. Tashkun, J. Tennyson, R.A. Toth, A.-C. Vandaele, J. Vander Auwera, J. Quant. Spectrosc. Radiat. Transfer 112 (2011) 2395–2445.
[21] H.M. Pickett, R.L. Poynter, E.A. Cohen, M.L. Delitsky, J.C. Perason, H.S.P. Muller, J. Quant. Spectrosc. Radiat. Transfer 60 (1998) 883–890.
[22] J.-M. Hartmann, C. Boulet, D. Robert, Collisional Effects on Molecular Spectra. Laboratory Experiments and Models, Consequences for Applications, Elsevier, New York, 2008.
[23] G. Cazzoli, L. Cludi, G. Cotti, C. Degli Esposti, G. Buffa, O. Tarrini, J. Chem. Phys. 102 (1995) 1149–1156.
[24] P. Duggan, P.M. Sinclair, R. Berman, A.D. May, J.R. Drummond, J. Mol. Spectrosc. 186 (1997) 90–98.
[25] (a) R. Ciuriło, A.S. Pine, J. Quant. Spectrosc. Radiat. Transfer 67 (2000) 375–393; (b) R. Ciuriło, A.S. Pine, J. Szudy, J. Quant. Spectrosc. Radiat. Transfer 68 (2001) 257–271.
[26] (a) G. Buffa, L. Dore, F. Tinti, M. Meuwly, ChemPhysChem 7 (2006) 1764–1769; (b) G. Buffa, L. Dore, F. Tinti, M. Meuwuly, ChemPhysChem 9 (2008) 2237–2244; (c) G. Buffa, O. Tarrini, L. Dore, M. Meuwly, ChemPhysChem 11 (2010) 3141–3145.
[27] (a) N. Tasinato, G. Duxbury, N. Langford, K.G. Hay, J. Chem. Phys. 132 (2010) 044316; (b) N. Tasinato, K.G. Hay, N. Langford, G. Duxbury, D. Wilson, J. Chem. Phys. 132 (2010) 164301; (c) G. Duxbury, N. Tasinato, K. Hay, D. Wilson, N. Langford, AIP Conf. Proc. 1290 (2010) 194–203.
[28] J.H. Butler, Geophys. Res. Lett. 21 (1994) 185–188.
[29] R.J. Cicerone, Science 263 (1994) 1243–1244.
[30] M.B. McElroy, R.J. Salawitch, S.C. Wosfy, J.A. Logan, Lett. Nat. 321 (1986) 759–762.
[31] M.J. Kurylo, J.M. Rodriguez, World Meteorological Organization (WMO), "Scientific Assessment of Ozone Depletion: 1998" Report 44, WMO Global Ozone Research and Monitoring Project, Chapter 2, Geneva, Switzerland, 1999.
[32] G. Graner, J. Mol. Spectrosc. 90 (1981) 394–438.
[33] R. Anttila, C. Betrencourt-Stirnemann, J. Dupré, J. Mol. Spectrosc. 100 (1983) 54–74.
[34] E. Brunetaud, I. Kleiner, N. Lacome, J. Mol. Spectrosc. 216 (2002) 30–47.
[35] F. Kwabia Tchana, I. Kleiner, J. Orphal, N. Lacome, O. Bouba, J. Mol. Spectrosc. 228 (2004) 441–452.
[36] F. Kwabia Tchana, D. Jacquemart, N. Lacome, I. Kleiner, J. Orphal, J. Mol. Spectrosc. 235 (2006) 132–143.
[37] D. Jacquemart, F. Kwabia Tchana, N. Lacome, I. Kleiner, J. Quant. Spectrosc. Radiat. Transfer 105 (2007) 264–302.
[38] D. Jacquemart, H. Tran, J. Mol. Spectrosc. 109 (2008) 569–579.
[39] L. Gomez, D. Jacquemart, J.-P. Bouanich, Z. Boussetta, H. Aroui, J. Quant. Spectrosc. Radiat. Transfer 111 (2010) 1252–1261.
[40] Z. Boussetta, H. Aroui, D. Jacquemart, L. Gomez, J.-P. Bouanich, J. Quant. Spectrosc. Radiat. Transfer 112 (2011) 769–778.
[41] K.J. Hoffman, P.B. Davies, J. Mol. Spectrosc. 254 (2009) 69–77.
[42] F. Kwabia Tchana, M. Ngom, A. Perrin, J.-M. Flaud, W.J. Lafferty, S.A. Ndiaye, El.A. Ngom, J. Mol. Spectrosc. 292 (2013) 1–4.
[43] M. Ngom, J.-M. Flaud, F. Kwabia Tchana, W.J. Lafferty, X. Landsheere, A. Perrin, El.A. Ngom, Can. J. Phys. 91 (11) (2013) 906–909.
[44] F. Kwabia Tchana, J.-M. Flaud, W.J. Lafferty, M. Ngom, Mol. Phys. 112 (2014) 1633–1638.
[45] W.H. Press, S.A. Teukolsky, W.T. Vetterling, B.P. Flannery, Numerical Recipes in C, second ed., Cambridge Univ. Press, Cambridge, MA, 1994.
[46] V. Dana, J.Y. Mandin, J. Quant. Spectrosc. Radiat. Transfer 48 (1992) 725–731.
[47] R.H. Dicke, Phys. Rev. 89 (1953) 472–473.
[48] J.M. Hartmann, C. Boulet, D. Robert, Collisional Effects on Molecular Spectra. Laboratory Experiments and Models, Consequences for Applications, Elsevier, Amsterdam, 2008.
[49] C. Bray, D. Jacquemart, N. Lacome, M. Guinet, A. Cuisset, S. Eliet, F. Hindle, G. Mouret, F. Rohart, J. Buldyreva, J. Quant. Spectrosc. Radiat. Transfer 116 (2013) 87–100.
[50] J. Ballard, R.J. Knight, J. Vander Auwera, M. Herman, G. Di Lonardo, G. Masciarelli, et al., J. Quant. Spectrosc. Radiat. Transfer 66 (2000) 109–128.
[51] J.P. Bouanich, G. Blanquet, J. Quant. Spectrosc. Radiat. Transfer 40 (1988) 205–220.
[52] J. Pourcin, A. Jacquemoz, A. Fournel, H. Sielmann, J. Mol. Spectrosc. 90 (1981) 43–50.
[53] G. Graner, W.E. Blass, J. Phys. France 36 (1975) 769–771.
[54] D. Reuter, D.E. Jennings, J.W. Brault, J. Mol. Spectrosc. 115 (1986) 294–304.
[55] V. Nemtchinov, K. Sung, P. Varanasi, J. Quant. Spectrosc. Radiat. Transfer 83 (2004) 243–265.
[56] A. Predoi-Cross, K. Hambrook, S. Brawley-Tremblay, J.P. Bouanich, V. Malathy Devi, M.A.H. Smith, J. Mol. Spectrosc. 236 (2006) 75–90. 2006.
[57] A. Predoi-Cross, K. Hambrook, S. Brawley-Tremblay, J.P. Bouanich, V. Malathy Devi, M.A.H. Smith, J. Mol. Spectrosc. 235 (2006) 35–53. 2006.
[58] A. Barbouchi Ramchani, D. Jacquemart, M. Dhib, H. Aroui, J. Quant. Spectrosc. Radiat. Transfer 120 (2013) 1–15.